












Changes in patterns of age-related network connectivity are associated with risk for schizophrenia

Roberta Passiatore^{a,b,c} , Linda A. Antonucci^a, Thomas P. DeRamus^b, Leonardo Fazio^d , Giuseppe Stolfa^a, Leonardo Sportelli^{a,e}, Gianluca C. Kikidis^{a,e} , Giuseppe Blasj^{a,f} , Qiang Chen^e , Juergen Dukart^{c,g}, Aaron L. Goldman^e, Venkata S. Mattay^{a,h}, Teresa Popolizioⁱ, Antonio Rampino^{a,f} , Fabio Sambataro^j, Pierluigi Selvaggi^{a,f}, William Ulrich^e, Apulian Network on Risk for Psychosis^{a,k,l,m,n,o}, Daniel R. Weinberger^{e,h,p,q,r} , Alessandro Bertolino^{a,f,1}, Vince D. Calhoun^{b,1} , and Giulio Pergola^{a,e,p,1} 

Edited by Helen Mayberg, Icahn School of Medicine at Mount Sinai, New York, NY; received December 19, 2022; accepted May 24, 2023

Alterations in fMRI-based brain functional network connectivity (FNC) are associated with schizophrenia (SCZ) and the genetic risk or subthreshold clinical symptoms preceding the onset of SCZ, which often occurs in early adulthood. Thus, age-sensitive FNC changes may be relevant to SCZ risk-related FNC. We used independent component analysis to estimate FNC from childhood to adulthood in 9,236 individuals. To capture individual brain features more accurately than single-session fMRI, we studied an average of three fMRI scans per individual. To identify potential familial risk-related FNC changes, we compared age-related FNC in first-degree relatives of SCZ patients mostly including unaffected siblings (SIB) with neurotypical controls (NC) at the same age stage. Then, we examined how polygenic risk scores for SCZ influenced risk-related FNC patterns. Finally, we investigated the same risk-related FNC patterns in adult SCZ patients (oSZ) and young individuals with subclinical psychotic symptoms (PSY). Age-sensitive risk-related FNC patterns emerge during adolescence and early adulthood, but not before. Young SIB always followed older NC patterns, with decreased FNC in a cerebellar–occipitoparietal circuit and increased FNC in two prefrontal–sensorimotor circuits when compared to young NC. Two of these FNC alterations were also found in oSZ, with one exhibiting reversed pattern. All were linked to polygenic risk for SCZ in unrelated individuals (R^2 varied from 0.02 to 0.05). Young PSY showed FNC alterations in the same direction as SIB when compared to NC. These results suggest that age-related neurotypical FNC correlates with genetic risk for SCZ and is detectable with MRI in young participants.

functional network connectivity | schizophrenia | neurodevelopment | familial risk | polygenic risk

Human brain maturation extends after adolescence well into the third decade of life and probably beyond (1). The period from late adolescence to adulthood is characterized by refinements of the structure and changes in functional connections of brain regions, such as the prefrontal cortex (PFC), with further maturation during the third decade of life (2, 3). Notably, late adolescence and early adulthood is also the period during which adult psychotic disorders, including schizophrenia (SCZ), have their typical clinical onset (4).

The neurodevelopmental hypothesis for the pathophysiology of SCZ (5) suggests that brain alterations during early life reflect pathogenic mechanisms, clinically silent until disease onset, which interact with neurotypical brain maturational events that occur many years later, facilitating the emergence of the SCZ syndrome. Functional magnetic resonance (fMRI) studies frequently reported alterations in functional network connectivity (FNC) in patients with SCZ compared with neurotypical individuals (NC), especially regarding PFC, that have also been associated with symptoms in the psychosis spectrum even before the onset (6).

This framework suggests that maturational brain processes occurring before the clinical onset may be linked with genetic and clinical risk for SCZ. The heritability of FNC varies from 20 to 60%, depending on the brain region considered (7, 8). Accordingly, SIBs show intermediate brain characteristics between NC and SCZ: SIB on average have lower FNC than NC, but greater FNC than patients with SCZ during resting-state or working memory performance (7, 9). Therefore, these FNC patterns may be heritable and cosegregate with genetic risk. For example, developmental trajectories of frontoparietal connectivity (10) have been hypothesized to underlie the onset of SCZ (11, 12), consistently with the observation that frontoparietal functional alterations are also present in unaffected siblings (SIB) of patients with SCZ, who, on average, share 50% of genetic variation with their affected sibling (13, 14). Although these differences may represent a potential intermediate phenotype of risk, to the extent that the functional brain changes in patients with SCZ are familial, only molecular estimates can establish whether the risk is genetic and

Significance

Are age-related changes in brain functional network connectivity (FNC) involved in schizophrenia (SCZ) risk? We measured FNC from childhood to adulthood across multiple fMRI acquisitions in 7,431 neurotypical individuals (NC), 201 first-degree relatives of patients with SCZ, of which 156 siblings (SIB), 195 patients with SCZ, and 1,409 individuals with subthreshold psychotic symptoms (PSY). Young SIB are characterized by early FNC alterations in prefrontal–sensorimotor and cerebellar–occipitoparietal circuits; these FNC patterns are associated with polygenic risk for SCZ. Two of these alterations were found in SCZ patients, one showed inverse patterns. Young PSY show the same patterns. Risk-related FNC patterns always resemble those of older healthy persons, whereas older SIB patterns approach the NC distribution once their age-evolving patterns reach maturity.

Competing interest statement: A.B. received consulting fees from Biogen and lecture fees from Otsuka, Janssen, and Lundbeck. D.R.W. serves on the Scientific Advisory Boards of Sage Therapeutics and Pasithea Therapeutics. G.B. received lecture fees from Lundbeck. A.R. received travel fees from Lundbeck. All other authors have no biomedical financial interests or potential conflicts of interest.

This article is a PNAS Direct Submission.

Copyright © 2023 the Author(s). Published by PNAS. This article is distributed under [Creative Commons Attribution-NonCommercial-NoDerivatives License 4.0 \(CC BY-NC-ND\)](https://creativecommons.org/licenses/by-nc-nd/4.0/).

¹To whom correspondence may be addressed. Email: alessandro.bertolino@uniba.it, vcalhoun@gsu.edu, or giulio.pergola@uniba.it.

This article contains supporting information online at <https://www.pnas.org/lookup/suppl/doi:10.1073/pnas.2221533120/-/DCSupplemental>.

Published August 1, 2023.

not associated with environmental risk factors shared between family members.

Genome-wide association studies (GWASs) have proven effective to identify common genetic risk variants according to a polygenic model (15–17). The polygenic risk score (PRS), which sums up the minor impacts of several common variants, can be used to evaluate the aggregated risk borne by genetic variants associated with the disorders among individuals (15). The PRS for SCZ is associated with brain FNC, especially involving prefrontal functional networks (18–20). However, the reported effect sizes are often small, and replications in independently collected samples have frequently failed (8). One possible explanation for PRSs' poor explanatory power on neuroimaging measures is that a single fMRI session may be a poor evaluation of a trait, resulting in low reproducibility (21, 22) and heritability (8). Previous studies have often used resting state to derive individual measures of FNC, although resting-state FNC presumably covers a limited portion of the impact of the polygenic risk on brain processes associated with SCZ (8, 18). Indeed, the reliability of FNC is highly dependent on the amount of data available (23, 24), with better heritability estimates of FNC achieved by integrating resting state and task data (25). Thus, combining multiple fMRI paradigms may improve the investigation of the influence of PRSs on brain FNC by accounting for the limitations of single modalities (26). It is also worth noting that PRSs are generated to discriminate diagnosis and only explain in toto approximately 7% of the liability to SCZ (16). Even though biological traits genetically cosegregating with SCZ liability may have a less complex genetic architecture and thus larger association effect sizes (27, 28), the existing literature has generally shown that associations of PRSs with traits genetically correlated with SCZ are likely to be a fraction of the 7% explained on the trait PRSs are meant to predict.

Studies combining multiple task-evoked fMRI modalities in adults have consistently revealed age-related (29) and disease-related FNC patterns (30) through independent component analysis (ICA) (29–31). ICA-based methods are data-driven strategies that capture activation covariance between regions, even across multiple fMRI modalities, and are used to measure FNC (32). Importantly, if FNC patterns are invariant across resting state and task-evoked fMRI modalities, then such patterns are possibly intrinsic to an individual and do not depend exclusively on a specific neuroimaging session or cognitive task condition (25). Indeed, task-related FNC departing from resting-state patterns likely represents the online use of brain resources for cognition, such that two regions may show coordinated activity, i.e., significant FNC, while they are both activated during task performance or while they are both inactivated during resting state or vice versa. This permits FNC to have the same direction throughout rest and task engagement, as opposed to activity, which is typically opposing between the two. Instead, brain regions that deviate from resting-state FNC during task engagement are likely switching networks to support task engagement. Therefore, combining task-related and resting-state FNC can measure individual differences in intrinsic FNC as well as dynamic changes (25).

Developmental alterations in FNC have also been reported through brain age approaches in individuals presenting attenuated or subthreshold psychotic symptoms (PSY), thus, considered at clinical risk for psychosis (33, 34). The PSY condition indicates an increased probability of a diagnosis of a psychotic disorder within the first 3 y following clinical presentation relative to the general population; the risk increases gradually during this period (35). The presentation of potentially prodromal symptoms happens mainly during late adolescence and early adulthood (35). Brain age studies using MRI data to capture changes in brain development and

quantify the gap between chronological age and brain-estimated age have consistently revealed older predicted age in SCZ (36, 37). Recently, Truelove-Hill et al. (38) showed that increased brain age assessed on resting-state and structural MRI is associated with subthreshold PSY in the Philadelphia Neurodevelopmental Cohort Study (PNC) (39). They did not study task-based activations. Additionally, FNC alterations during adolescence have been associated with compromised mental health in adulthood (40). Thus, FNC has the potential to characterize genetic risk for SCZ that may thwart development in a psychosis trajectory. We hypothesize that brain alterations in PSY, many of whom already have manifest features of psychosis or are likely to approach developmental end points characteristic of psychosis spectrum disorders, might present the same patterns of FNC as individuals at genetic risk for SCZ.

We set out to study functional brain changes occurring between early and later adulthood that may reveal age-related brain mechanisms relevant to SCZ risk using multiple fMRI paradigms. We investigated FNC patterns in a cross-sectional framework on a total of 9,236 individuals through a fully automated ICA pipeline called NeuroMark, using spatial references from the NeuroMark_fMRI_1.0 template (41) on resting state, working memory, episodic memory, and emotion recognition tasks during fMRI. Six different cohorts have been analyzed, one provided by the Lieber Institute of Brain Development (LIBD), one obtained from the publicly available PNC (39), two independent cohorts acquired at the University of Bari Aldo Moro (UNIBA), one obtained from the Adolescent Brain Cognitive DevelopmentSM (ABCD), and one from the UK Biobank (UKB). We divided individuals into three age stages, i.e., from 8 to 14 y old (“children,” marked by a lowercase “c”; the vast majority were between 9 and 11 y old), from 15 to 25 y old (“younger” individuals, marked by a lowercase “y”), and from 30 to 60 y old (“older” individuals, marked by a lowercase “o”) relying on the SCZ risk and clinical manifestations' trajectory (35, 42). To improve discrimination between developing and mature brains, we left out samples aged 25 to 30 y (43), as risk-related brain functional characteristics are likely to interact with brain maturation that for some brain regions like the PFC end around 25 y old (1, 5).

First, we sought to identify age-related FNC pattern changes in early adulthood by comparing yNC and oNC using separate linear mixed-effect models on each individual independent component (IC) pair Pearson's correlation that reflects the relationship between any two ICs. Then, we hypothesized that age-varying FNC patterns are associated with familial risk for SCZ. We analyzed FNC patterns in SIB matched with NC for age stage. We compared data from children and young groups to estimate whether risk-related FNC patterns emerge during childhood or later during adolescence. Furthermore, we tested the association between FNC patterns altered in SIB and PRS for SCZ (16), hypothesizing that FNC alterations associated with the risk of developing SCZ are heritable. We also investigated FNC in oSCZ for clinical validation of the FNC patterns detected. Finally, we assessed the early detection potential of risk-related FNC patterns investigating young PSY. Fig. 1 depicts the outline of the study.

1. Results

1.1. Characterization of Age-Related Neurotypical Functional Connectivity Patterns. We characterized nine different groups: NC children (cNC, $N = 3,726$), younger neurotypical adults (yNC, $N = 757$), older neurotypical adults (oNC, $N = 2,948$), children SIB ($N = 17$), children FHR ($N = 45$) considered together as cSIB/FHR, younger SIB (ySIB, $N = 53$), older SIB (oSIB, $N = 86$),

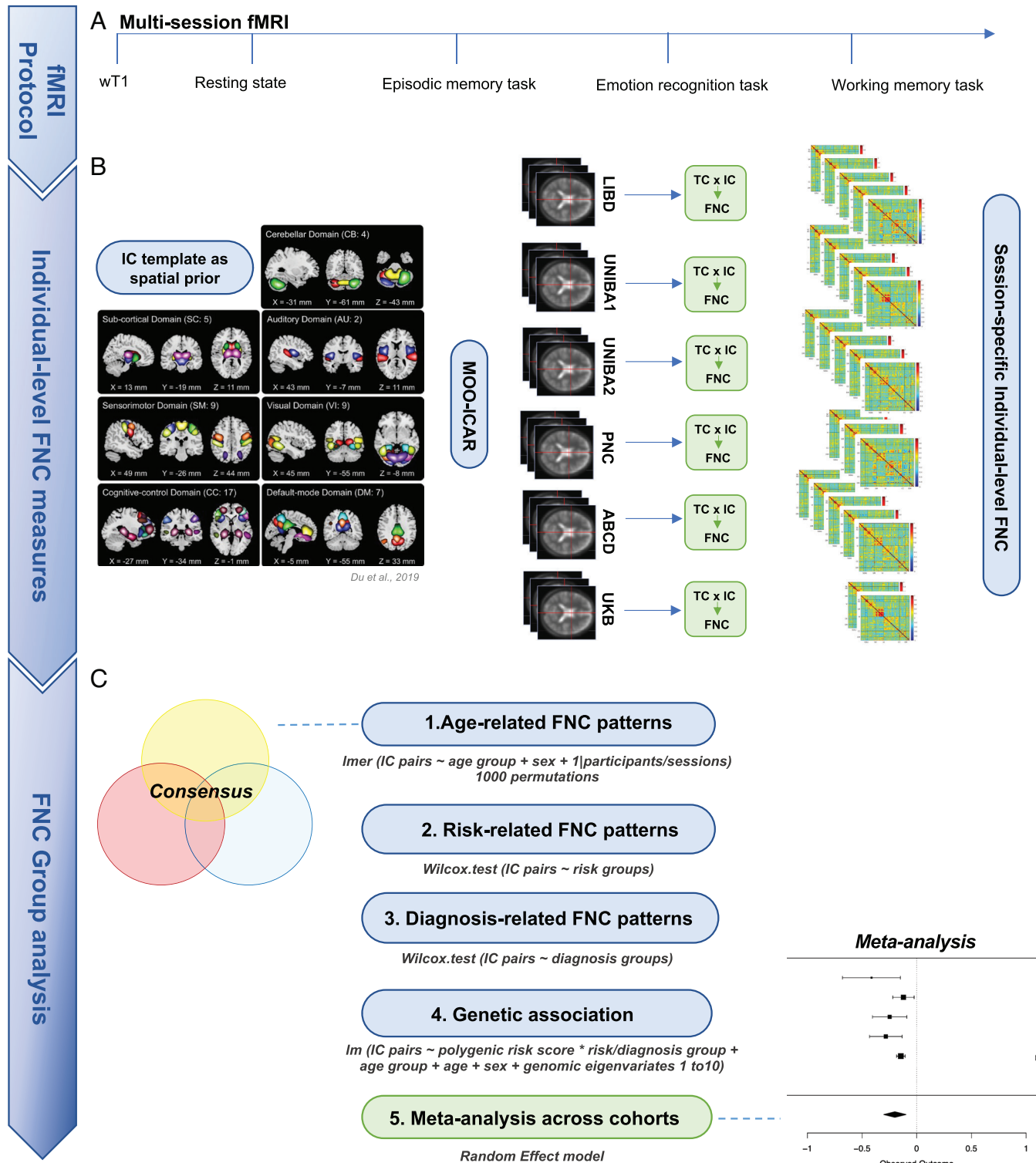


Fig. 1. Chart describing the outline of this study including (A) the multisession fMRI protocol, (B) the individual-level FNC matrices determination through the application of the MOO-ICAR Algorithm [Du et al. (41)] on each fMRI session, (C) the group analysis on (1) the age-related FNC, (2) the familial risk-related FNC and, subsequently, the clinical risk-related FNC, (3) the SCZ-related FNC, (4) the genetic analysis PRS × FNC across groups within cohorts, and (5) the meta-analysis on the association PRS × FNC across cohorts.

PSY children (cPSY, N = 1,284), younger PSY (yPSY, N = 125), and older patients with SCZ (oSCZ, N = 195). The sample size determination and demographic characteristics of all cohorts are described in *Materials and Methods*, Section 4.1, and Table 1. Also, see *SI Appendix, section 1*, for a complete description of recruitment, data collection procedures, and exclusion criteria.

We performed a multiobjective optimization ICA with spatial reference (MOO-ICAR) (44) and analyzed age-related FNC patterns using separate linear mixed-effect models for each IC pair, hence investigating connectivity between functional networks. Of 1,370 IC pairs, the consensus across cohorts showed 17 IC pairs covering the cerebellar (N = 2 IC pairs), cognitive control

Table 1. Demographic characteristics and treatment data for individuals selected for the analysis from the LIBD, UNIBA1, UNIBA2, PNC, ABCD, and UKB cohorts

Cohort	Group	N	Mean age \pm SD in years (range)	%Male	Mean chlorpromazine equivalents \pm SD in mg/day
LIBD	yNC	200	22 \pm 2 (18:25)	42	/
	oNC	246	41 \pm 7 (30:56)	47	/
	ySIB	41	21 \pm 2 (18:25)	68	/
	oSIB	40	42 \pm 8 (30:60)	41	/
	oSCZ	88	40 \pm 8 (30:56)	59	258 \pm 221 (N = 54)
UNIBA 1	yNC	356	22 \pm 2 (18:25)	39	/
	oNC	125	39 \pm 7 (30:60)	62	/
	ySIB	12	22 \pm 2 (17:25)	30	/
	oSIB	46	40 \pm 6 (30:59)	41	/
	oSCZ	82	38 \pm 6 (30:58)	45	219 \pm 151 (N = 54)
UNIBA 2	yNC	127	22 \pm 1 (17:25)	37	/
	oNC	57	35 \pm 6 (30:59)	63	/
	yPSY	46	20 \pm 3 (16:25)	47	/
	oSCZ	25	37 \pm 6 (30:50)	64	182 \pm 96 (N = 20)
PNC	cNC	90	11 \pm 2 (8:14)	47	/
	cPSY	44	12 \pm 1 (9:14)	59	/
	yNC	74	17 \pm 2 (15:23)	55	/
	yPSY	79	17 \pm 2 (15:23)	34	/
ABCD	cNC	3,636	9.9 \pm 1 (9:11)	47	/
	cSIB/FHR	62	9.9 \pm 1 (9:11)	53	/
	cPSY	1,238	9.8 \pm 1 (9:11)	24	/
UKB	oNC	2,520	53 \pm 6 (40:60)	47	/

(N = 7 IC pairs), default mode (N = 4 IC pairs), sensorimotor (N = 2 IC pairs), subcortical (N = 2 IC pairs), and visual (N = 5 IC pairs) circuits (empirical *P* value of such a high consensus across cohorts 1×10^{-4} , Fig. 2). Specifically, we found that oNC showed reproducibly greater FNC compared to yNC within the anterior default mode network, between sensorimotor, medial PFC, and dorsolateral PFC, respectively, Brodmann Area (BA) 8 and 9, between the striatum and medial temporal lobe, and between parietal and occipital cortices [false discovery rate significance correction (45)—*pFDR* < 0.05]. oNC showed decreased FNC compared with yNC within the posterior default mode network, between the cerebellum, hippocampus, and occipital cortices, and between the anterior default mode network and the striatum (*pFDR* < 0.05).

We also considered the age group \times session interaction in the previously described linear mixed-effect models for each IC pair to assess whether FNC differences between yNC and oNC are reliant on a single fMRI session. None of the 17 age-related IC pairs in which we found age differences considering all sessions showed a significant age groups \times session interaction, as well as no age group \times session significant interactions have been reported (*P* < 0.05). Further details about the age group \times session interaction analysis are reported in *SI Appendix, section 6.1*.

To study whether age-related neurotypical FNC patterns were associated with behavioral performance, we tested the relationship between averaged FNC patterns across multiple fMRI acquisitions and i) hit rate and ii) RT at the working memory task, and the same measures at retrieval during the episodic memory task. No associations survived correction for multiple comparisons (*pFDR* < 0.05). Behavioral performance collected during working and episodic memory tasks is shown in *SI Appendix, Table S3*. See *SI Appendix, sections 2 and 3*, for further details about the experimental procedure and *Materials and Methods*, Section 4.4, for

further details about the association between FNC with behavioral indices.

1.2. Characterization of Familial Risk-Related Functional Connectivity Patterns in SIB. To test the hypothesis of altered FNC patterns associated with familial risk for SCZ, we used the Wilcoxon signed-rank test and compared yNC and ySIB FNC patterns in each cohort. See *Materials and Methods*, Section 4.5, for a detailed description. We found a significant difference in three of the 17 consensus age-associated IC pairs. Specifically, ySIB showed decreased FNC between a cerebellar–occipital–parietal circuit compared with yNC ($w = 0.08$; *pFDR* = 3×10^{-4} ; Fig. 3*A*). Moreover, ySIB showed increased FNC both within a medial PFC–sensorimotor circuit ($w = 0.24$; *pFDR* = 2×10^{-4} ; Fig. 3*B*) and a dorsolateral PFC–sensorimotor circuit ($w = 0.25$; *pFDR* = 2×10^{-4} ; Fig. 3*C*). Regarding the older adults' groups, oSIB and oNC showed no significant differences in the cerebellar–occipitoparietal and dorsolateral PFC–sensorimotor circuits FNC (respectively, $w = 0.05$; *pFDR* = 0.19 and $w = 0.01$; *pFDR* = 0.60; Fig. 3*A* and *C*), whereas, similar to ySIB, oSIB showed increased FNC compared to oNC in the medial PFC–sensorimotor circuit ($w = 0.14$; *pFDR* = 1×10^{-4} , Fig. 3*B*). We also tested FNC differences between oNC and oSIB in the remaining 14 age-related IC pairs which showed no significant differences (*pFDR* > 0.05).

To backtrack FNC alterations during childhood, we tested cNC vs cSIB/FHR FNC differences in the ABCD cohort for the three IC pairs in which we found age- and familial risk-related alterations. Results showed no significant differences during childhood (*pFDR* > 0.05; Fig. 3). Further details are reported in the *SI Appendix, section 6.2*.

To examine whether risk-related FNC patterns were significantly associated with polygenic risk for SCZ, we investigated the

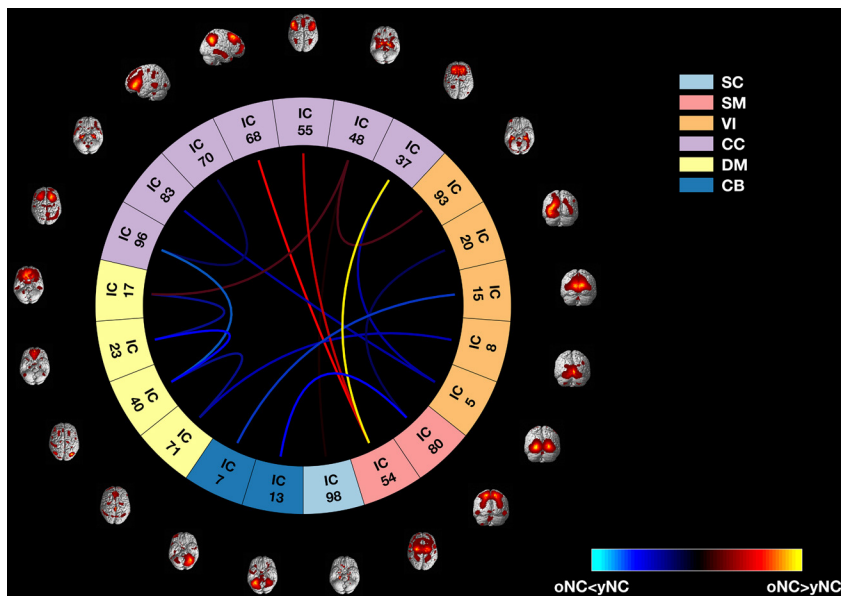


Fig. 2. Connectome plot showing the differences between yNC and oNC on FNC estimated on multiple fMRI sessions among age-related IC pairs resulted from the consensus across the LIBD, UNIBA1, and UNIBA2 cohorts. The 17 IC pairs included in the cerebellar (CB, $N = 2$), cognitive control (CC, $N = 7$), default mode (DM, $N = 4$), sensorimotor (SM, $N = 2$), subcortical (SC, $N = 2$), and visual (VI, $N = 5$) networks. Blue lines represent decreased FNC in oNC compared with yNC, whereas red lines represent increased FNC in oNC compared with yNC.

relationship between the averaged FNC patterns across sessions and PRS (15) in all the individuals included, with diagnosis and age group as a factor of no interest in the analysis in interaction with the PRS. We tested 10 PRSs (PRS1 to 10) based on ten thresholds of association with SCZ diagnosis according to the original approach taken by Trubetsky et al. (16) and accounted for multiple comparisons through pFDR significance correction. See *Materials and Methods*, Section 4.6, for a detailed description. Mixed-effect model meta-analysis across cohorts showed a significant positive association between the medial PFC–sensorimotor circuit and the PRS1 ($r = 0.13$; $pFDR = 1.35 \times 10^{-7}$; Fig. 4B), PRS2 ($r = 0.12$; $pFDR = 1.63 \times 10^{-7}$; Fig. 4B), and PRS3 ($r = 0.14$; $pFDR = 7.46 \times 10^{-8}$; Fig. 4B) and between the dorsolateral PFC–sensorimotor circuit

and PRS1 ($r = 0.16$; $pFDR = 2.97 \times 10^{-4}$; Fig. 4C) and PRS2 ($r = 0.14$; $pFDR = 1.27 \times 10^{-3}$; Fig. 4C), as well as a significant negative association between cerebellar–occipitoparietal FNC with PRS1 ($r = -0.20$; $pFDR = 8.45 \times 10^{-4}$; Fig. 4A) and PRS2 ($r = -0.21$; $pFDR = 8.69 \times 10^{-6}$; Fig. 4C). All directions were consistent with the effects detected in ySIB relative to yNC. No significant risk/diagnosis groups \times PRS has been found ($pFDR > 0.05$), while significant age groups \times PRS interactions have been found in the cerebellar–occipitoparietal circuit with PRS1 ($r = -0.14$; $pFDR = 0.02$) and the dorsolateral PFC–sensorimotor circuit with PRS3 ($r = 0.31$; $pFDR = 0.009$) and PRS4 ($r = 0.32$; $pFDR = 0.001$). In both cases, the effect size was larger for young than older individuals. See *SI Appendix*, section 6.3, for further details.

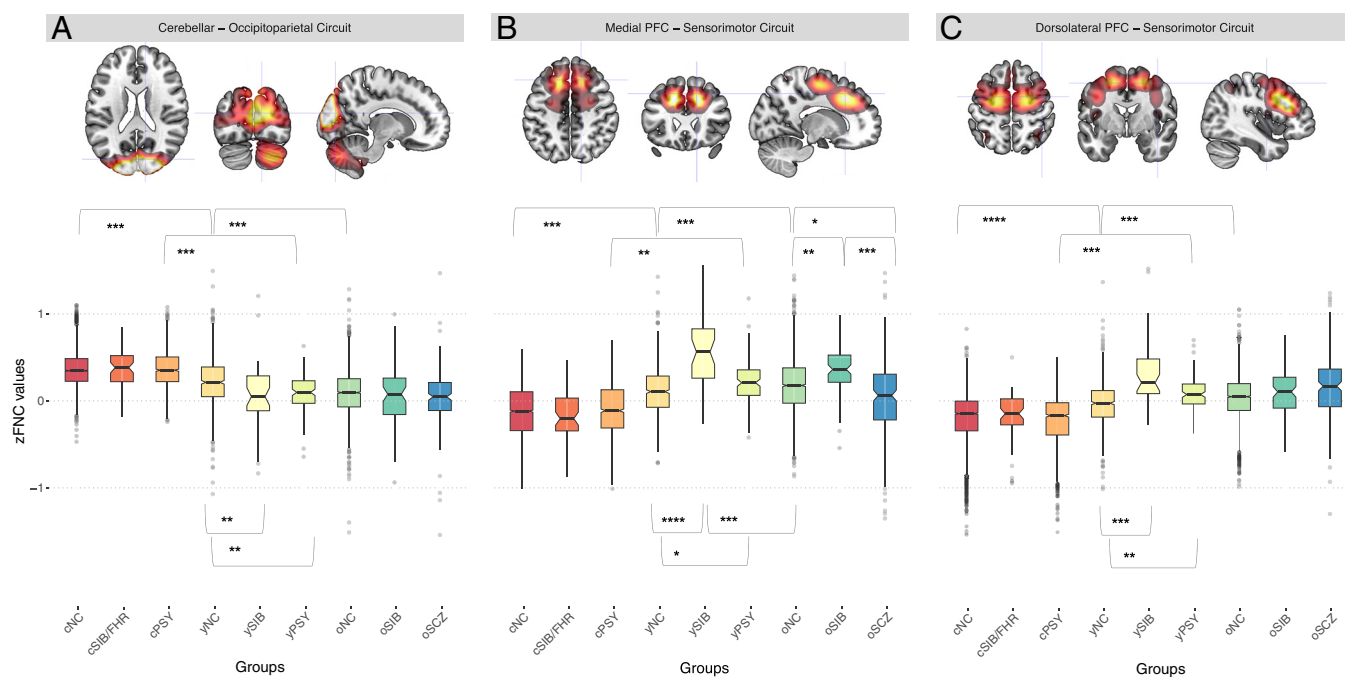


Fig. 3. Brain sections depicting the (A) cerebellar–occipitoparietal circuit and the (B) medial and (C) dorsolateral PFC circuits. Boxplots showing differences on averaged FNC across sessions among risk-related IC pairs comparing all groups, i.e., cNC, yNC, oNC, cSIB/FHR, ySIB, oSIB, cPSY, yPSY, and oSCZ. Significant differences in each of the three cohorts are indicated with asterisks. Different colors represent different groups: cNC (red), cSIB/FHR (orange), cPSY (light orange), yNC (dark yellow), ySIB (yellow), yPSY (light green), oNC (green), oSIB (dark green), and oSCZ (blue).

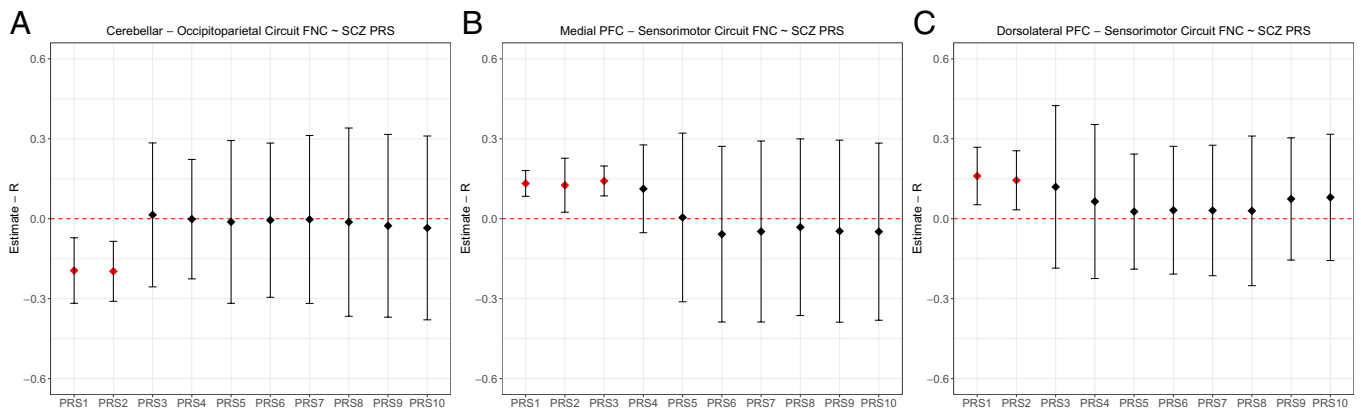


Fig. 4. Plots showing the association between polygenic risk for SCZ and FNC across sessions related to (A) the cerebellar–occipitoparietal circuit; (B) the medial PFC–sensorimotor circuit; and (C) the dorsolateral PFC–sensorimotor circuit. The threshold $pFDR < 0.05$ was considered on meta-analytic mixed-effect-model-derived P values extracted across cohorts (C.I. 0.95), accounting for multiple comparisons via Benjamini–Hochberg. Significant associations are reported in red.

1.3. Characterization of SCZ-Related Functional Connectivity Patterns.

To define altered FNC patterns associated with SCZ diagnosis compared with the age-related neurotypical FNC patterns, we used the Wilcoxon signed-rank test and compared oNC and oSCZ, oSIB vs oSCZ FNC patterns. FNC differed comparing oNC and oSCZ ($pFDR = 1.2 \times 10^{-8}$; Fig. 3A) in the medial PFC–sensorimotor circuit, but in the opposite direction as compared to risk-related FNC, i.e., oSCZ showed decreased FNC compared to oNC. Also, medial PFC–sensorimotor circuit FNC was different comparing oSIB and oSCZ ($pFDR = 2.3 \times 10^{-8}$; Fig. 3A). Except for this pattern showing counterintuitive results, the direction of effects in oSCZ was consistent with that of oSIB and oNC relative to yNC (Fig. 3), showing descriptively more extreme scores than NC and SIB.

We also analyzed the association between FNC and antipsychotic-based medication in a subsample of oSCZ with available treatment data (Table 1) to assess whether SCZ-related FNC patterns were possibly influenced by pharmacological treatment. However, no association was significant between antipsychotic-based medication in oSCZ and cerebellar–occipitoparietal FNC across cohorts ($r = -0.1$; P value = 0.09), as well as antipsychotic-based medication with medial PFC–sensorimotor FNC ($r = -0.04$; P value = 0.84) and with dorsolateral PFC–sensorimotor PFC ($r = -0.001$; P value = 0.98). Results are depicted in *SI Appendix*, Fig. S11. Further control analyses were conducted on FNC, structural metrics, and antipsychotic-based medication. Results are reported in *SI Appendix*, section 6.4.

1.4. Characterization of Clinical Risk-Related Functional Connectivity Patterns in PSY.

To define altered FNC patterns associated with the presence of subthreshold PSY compared with the age-related neurotypical FNC patterns, we used the Wilcoxon signed-rank test and compared yNC and yPSY FNC patterns in the UNIBA2 and PNC cohorts. yNC and yPSY showed a significant difference ($pFDR < 0.05$) in the same IC pairs that were also associated with the genetic risk for SCZ, with a consistent direction, i.e., yPSY showed lower FNC between the cerebellar–occipitoparietal circuit (Fig. 3A) compared with yNC ($pFDR = 1.40 \times 10^{-6}$). Moreover, yPSY showed higher FNC both within the medial PFC–sensorimotor circuit ($pFDR = 2.50 \times 10^{-5}$; Fig. 3B) and the dorsolateral PFC–sensorimotor circuit ($pFDR = 1.20 \times 10^{-7}$; Fig. 3C). No significant difference ($pFDR > 0.05$) was found between yPSY and oNC in the UNIBA 2 cohort, despite the age difference.

To estimate whether risk-related FNC emerges during childhood, we estimated the FNC patterns of cNC and cPSY included in the

PNC and ABCD cohorts. Also, cNC and yNC groups were compared to define age-related FNC changes in the cerebellar–occipitoparietal and medial and dorsolateral PFC–sensorimotor circuits in the PNC cohort. No significant clinical risk–related difference ($P > 0.05$) has been found between cNC vs cPSY FNC patterns; however, cNC and yNC FNC patterns significantly differed in the cerebellar–occipitoparietal circuit ($pFDR = 6.60 \times 10^{-7}$), in the medial ($pFDR = 1.10 \times 10^{-5}$) and dorsolateral PFC–sensorimotor ($pFDR = 8.70 \times 10^{-7}$) circuits, following the age-related change directions of yNC compared with oNC FNC patterns in the LIBD, UNIBA1, and UNIBA2 cohorts (Fig. 3).

2. Discussion

In this large cross-sectional study combining six different cohorts of a total of 9,236 unrelated individuals, we report age-related FNC pattern changes between 8 and 14, 15 and 25, and 30 and 60-y old individuals leveraging multiple fMRI acquisitions including resting state, working memory, episodic memory, and emotion recognition tasks. Age-related differences are mirrored in ySIB in the same direction as oNC patterns. The generally decreasing difference between SIB and NC with age supports an early manifestation of FNC patterns associated with familial risk for SCZ rather than a lifelong stable trait. The familial risk–related FNC patterns are replicated in the analysis on the polygenic risk for SCZ suggesting the consistency of these results with the genetic underpinnings of SCZ. Furthermore, oSCZ FNC exhibits the same patterns of alteration in two of the three patterns identified, implying that these age-related features also characterize the disorder itself. Finally, the altered FNC patterns found in yPSY preliminarily suggest that intrinsic FNC patterns observed via fMRI could be investigated as early detection markers.

2.1. Characterization of Age-Related Neurotypical Functional Connectivity Patterns.

We employed a three-age grouping founded on the SCZ risk and clinical manifestations trajectory to define FNC patterns associated with age stages, characterizing differences in terms of system-level FNC. FNC measured using fMRI, however, does not directly reflect the underlying structure of neuronal networks. Instead, FNC reflects signal coupling between brain regions without implying that greater coupling is more or less functional. In this scenario, older adults are characterized by both decreases and increases in FNC of PFC compared with younger adults (46). Discrepant findings often depend on the fMRI data analyzed, i.e., resting-state vs. cognitive tasks

(47, 48). Nonetheless, our findings support previous evidence showing an age-related increase in FNC in the PFC (49). In our investigation, the FNC between the PFC and sensorimotor cortices increased with age, whereas it decreased between the cerebellum, hippocampus, parietal and occipital cortices, and the anterior default mode network and striatum. The presence of both default mode and task active brain regions is a reminder that FNC, unlike activity, may well follow the same direction across task engagement and resting state. Also, previous studies have shown FNC variations associated with age within corticocerebellar networks during resting state or the performance of working memory tasks (50). Although the cerebellum is generally linked with motor processes, it also contributes to executive function, memory, and language (51, 52).

Indeed, previous studies suggested age-related changes in FNC as a compensatory mechanism in association with age-related decline in adults in terms of cognitive performance (53). Here, we found no significant correlation with cognitive performance during fMRI acquisition. Unfortunately, working and episodic memory performance data during fMRI were available only for a small portion of the individuals included in the LIBD, UNIBA1, and UNIBA2 cohorts (35% on average), while only working memory performance was available for PNC and ABCD individuals and none for UKB based on the task fMRI protocols acquired. Thus, we cannot speculate on the functional meaning of these results. Furthermore, because the estimated FNC is based on numerous task-active and resting-state sessions, performance in specific tasks may be inconsistent with the underlying FNC patterns found across multiple fMRI sessions. The relationship of cognitive assessments with these FNC patterns is likely to require more statistical power than our study provided.

2.2. Characterization of Familial Risk-Related Functional Connectivity Patterns. Multisession fMRI shows that age-varying FNC patterns are altered in familial risk for SCZ. In components where an age-group effect has been detected, alterations in FNC related to familial risk for SCZ show anticipatory FNC maturation patterns. Specifically, ySIB exhibited decreased FNC within a cerebellar–occipitoparietal circuit compared to neurotypical individuals of the same age, as well as increased FNC across medial PFC–sensorimotor and dorsolateral PFC–sensorimotor circuits. Previous research has associated SCZ with PFC impairment, mainly during resting state or working memory tasks (10, 54, 55). The PFC is a critical component of the neural circuitry that underpins executive functions such as planning, working memory, and impulse control, which also coordinates higher-order cognitive processes and executive functioning (56). Notably, the PFC is also one of the latest brain regions to complete development (1). Here, we find that PFC connectivity alterations associated with risk for SCZ are intrinsic rather than specific to resting state or working memory, spanning across multiple fMRI sessions and cognitive domains.

It is noteworthy that while the cerebellum is among the first brain structures to begin cellular differentiation, it is also one of the last to fully mature (57). Cerebellar maturation implicates corticocerebellar circuit formation leading to decreased corticocerebellar FNC as individuals grow (57). As such, the developing cerebellum is vulnerable to alterations in the development of cortical targets during critical periods of circuit formation, i.e., childhood, adolescence, and early adulthood (58, 59). We found a steeper decrease of corticocerebellar connectivity in SIB and PSY relative to controls, suggesting a maladaptive FNC development.

Our finding that risk-associated FNC patterns phenomenologically resemble the FNC patterns of neurotypical individuals over a decade older complements previous studies showing a larger

brain age gap based on resting-state fMRI in neurodevelopmental trajectories associated with psychotic subthreshold symptoms compared with neurotypical brain age (37, 38, 60) in younger individuals between 8 and 21 y old in PNC, though using a different analytical approach. These differences do not necessarily match alterations in oSCZ FNC patterns, which we show to display higher variance plausibly related to nongenetic factors. Our results raise the possibility that the anticipated development of intrinsic and task unselective FNC patterns during adolescence and early adulthood is associated with familial and polygenic risk for SCZ. In two of the three patterns we detected, oSIB no longer differed from age-matched oNC. The exception was a reduced but still significant FNC difference between oSIB and oNC in the medial PFC–sensorimotor circuit. We propose two explanations for these findings. First, the anticipatory FNC changes observed in ySIB no longer progress during adulthood, although development in NC reaches the same patterns more slowly. It is worth noting that working and episodic memory, two of the four conditions studied, often diminish with age (61). In this light, the expected pattern seems to indicate a steeper decline rather than an accelerated development. Second, this finding reflects the depletion of risk-related FNC characteristics in individuals who have dodged their genetic risk for SCZ at an age when the psychotic onset is less frequent. In other words, the ySIB group is at a sixfold higher risk (62) than the yNC cohort at risk of developing psychosis spectrum disorders over the years following our study, a risk much lower in oSIB. On the other hand, the permanence of altered patterns from youth to adulthood in SIB within the medial PFC–sensorimotor circuit, besides representing a replication of the effect, fits well in an intermediate phenotype framework.

Besides the significant FNC \times PRS associations in the medial PFC–sensorimotor circuit, the one showing the familial risk effect regardless of the age stage, FNC \times PRS interactions were significant in the two components with a difference between SIB and NC limited to young individuals. This result supports the idea that young SIBs show mainly anticipation of FNC patterns typical of older individuals and not an amplitude difference preserved across aging, reflected by significant age group \times PRS interactions. However, given the missing age stages in some of the cohorts we analyzed, this conclusion derives from three out of six cohorts and hence seems to us less solid than the consistent PRS associations across age stages from six independent cohorts. Nevertheless, this explorative analysis highlights the importance of windowing studies aimed to investigate SCZ risk: Age is a relevant factor to candidate SCZ risk phenotype manifestation (43).

Interestingly, the absence of differences across groups in the ABCD sample suggests that this pattern of FNC alteration occurs specifically in late adolescence–early adulthood and not earlier during childhood. This finding is in line with previous studies showing that brain connectivity alterations, specifically in the occipitotemporal cortex, were shared by patients with an early diagnosis of SCZ during adolescence and their healthy SIB, emerging only during adolescence (12 to 22 y old) and gradually normalizing during adulthood when compared to age-matched NC (63).

2.3. Characterization of SCZ-Related Functional Connectivity Patterns. Counterintuitively, the same medial PFC–sensorimotor circuit most reliably altered in SIB followed an opposite direction in oSCZ relative to oSIB. Critically, the PRS did not interact with diagnosis, meaning that it was preserved in the patient population in the same direction as in NC—suggesting that polygenic risk for SCZ did not account for this effect. We interpret this result in the context of extant reports of stable and transient alterations in sensorimotor circuits associated with treatment and symptom

improvement in patients with SCZ (64, 65). We did not find a significant antipsychotic dose effect in association with this FNC pattern; however, all patients with SCZ differ from NC in that they are medicated to compensate for their symptoms; therefore, the fact that patients do not significantly differ from each other cannot discount a difference between cases and controls driven by pharmacological treatment. Accordingly, Anticevic et al. (66) showed increased FNC in unmedicated patients at the first episode of psychosis compared with NC, specifically for the medial regions of the PFC. Interestingly, the authors reported that after 12 mo, patients were characterized by decreased FNC estimates, suggesting an inversion of FNC patterns associated with the course of the illness. Thus, this inverted FNC pattern in oSCZ may reflect the progressive brain changes present in chronic SCZ (66).

The heritability of the effects we identified is supported by the significant associations found between a PRS for SCZ and FNC patterns across groups. Multiple studies have reported the association between brain functional alterations and PRS (13, 18, 20, 67), but in addition in this report we suggest a possible brain developmental pattern of FNC associated with polygenic risk for SCZ in as many individuals and so consistent across cohorts. Some previous studies have reported higher correlations between functional brain phenotypes and PRS for SCZ, with R^2 ranging between 0.05 and 0.12 (18, 20), compared to our $R^2 \sim 0.02$ to 0.05. It is important to set appropriate expectations for these effect sizes because the effect of PRSs is more likely inflated in relatively small than large samples. Indeed, studies on larger samples showed lower correlations between functional brain phenotypes and PRS for SCZ, with R^2 ranging between 0.008 and 0.03 (67). The effect of the PRS on neuroimaging phenotypes of SCZ risk is a fraction of the entire heritability, which includes nonadditive and rare variant heritability. Heritability is, in its own right, a fraction of phenotypic variance. The comparison between SIB and NC, by definition, includes more heritability than the PRS. Note that the effect sizes estimated in our SIB vs. NC comparison range between 8 and 25% of the variance, thus much larger than PRS effects. Additionally, it is unlikely that a score developed to predict SCZ diagnosis may explain more than about 7% of the variance of any other phenotype (16). Instead, it could be expected that only some of the biological pathways represented in the PRS are associated with select phenotypes (68, 69). Given these considerations, the 2 to 5% of phenotypic variance explained by the PRS for SCZ in our study represents a considerable fraction of the plausible explainable heritability and is consistent with previous reports (18, 20).

Notably, we only found consistent changes in FNC patterns that were significantly associated with PRS by combining resting-state and task-evoked fMRI sessions. The effects found when analyzing each session separately did not reach statistical significance. As a result, we propose that estimating intrinsic FNC based on multisession fMRI captures the FNC associated with age-related evolution and psychopathological processes better than a single session, probably because multisession fMRI more reliably captures trait measures.

2.4. Characterization of Clinical Risk-Related Functional Connectivity Patterns. As regards the clinical high-risk condition for psychosis, yPSY showed decreased FNC within a cerebellar-occipital-parietal circuit compared with neurotypical individuals in the same age stage, as well as increased FNC between medial PFC–sensorimotor and dorsolateral PFC–sensorimotor circuits. Identifying risk patterns in SIBs can thus contribute to the characterization and detection of potential prodromal phases of chronic psychosis. It is noteworthy that the anticipated FNC patterns reported here and in other studies refer to a period after adolescence because, between birth and puberty,

neurodevelopment is generally delayed in individuals later diagnosed with SCZ (14, 70, 71).

In line with our findings in SIB, we found this pattern of FNC alteration specifically in late adolescence–early adulthood and not before during childhood as showed by the absence of differences across groups in the PNC and ABCD samples. These results suggest that the risk-related brain phenomenology is not yet detectable during childhood and instead unfolds in late adolescence–early adulthood. This evidence is in line with literature studying FNC in PSY during childhood, adolescence, and early adulthood (72, 73) and is consistent with a neurodevelopmental hypothesis framework (5), suggesting a potential venue for biomarker identification. Longitudinal studies will be needed to address whether the connectivity patterns associated with genetic risk that we highlighted here are also associated with higher transition rates in clinical high risk for psychosis.

2.5. Limitations. We analyzed cross-sectional data including individuals in three different age stages from six different cohorts. Some of the groups we compared showed differences in terms of age distribution (Table 1 and *SI Appendix, Fig. S1*). We opted to correct statistical models for age differences, rather than match for age across cohorts, to safeguard statistical power. In addition, only data from SCZ patients older than 30 y were available for the analysis, so it cannot be assumed that younger patients with SCZ show the same pattern.

From a methodological perspective, we used data from six different cohorts acquired with different MRI sequences and sometimes experimental procedures. For example, the episodic memory task acquired in the LIBD and UNIBA1 cohorts was a block-designed implicit encoding task; in contrast, the event-related task acquired in the UNIBA2 cohort was an explicit associative memory task. Also, the episodic memory task was not acquired at all in the PNC, ABCD, and UKB cohorts, as well as the N-back in the UKB. This aspect might have introduced a confounding effect that could favor consensus across cohorts in terms of averaged FNC while concealing further significant session-specific findings and reducing the power of genetic associations. In other words, the heterogeneity between cohorts makes these findings overly conservative, at the expense of sensitivity. The cohorts we employed included at least two of the three cognitive/affective domains we considered for most subjects, a factor limiting the availability of suitable publicly available datasets in the age range of our interest and the overall numerosity.

As brain aging has been reported to be strongly influenced by nongenetic factors like drug use, traumatization, and comorbid affective disorders (74–76), further studies should consider additional nongenetic factors, and potentially, gene–environment correlations and interactions (77–79) to complement our findings.

3. Conclusions

This study employed a multisession characterization of brain functional system interaction to test the hypothesis that FNC patterns characteristic of adulthood are aligned with familial or clinical risk for SCZ. Our findings suggest that an anticipated display of FNC patterns characteristic of older age is associated with a high risk for psychosis during late adolescence and early adulthood. As this is the stage of development during which psychotic symptoms might appear (80), the early detection of biased trajectories with MRI is potentially relevant to prevention strategies for individuals with liability for SCZ. The association of the same patterns with the polygenic risk for SCZ suggests that familial risk aligns with molecular estimates of polygenic risk. We propose that changes in FNC across cognitive tasks investigated in a longitudinal

framework may be further developed as early detection strategies in the effort to identify prodromal phases of SCZ.

4. Materials and Methods

4.1. Participants.

4.1.1. LIBD, UNIBA1, and UNIBA2. Participants were assessed in person with a Structured Clinical Interview for DSM-IV (SCID) (81). Inclusion/exclusion criteria are described in *SI Appendix, section 1*. Written informed consent was obtained after a full understanding of the protocol according to the Declaration of Helsinki. For the LIBD cohort, the experimental protocol was in accordance with the ethical standards of the NIH. For the UNIBA cohorts, the experimental protocol was approved by the institutional ethics committee of the UNIBA. As the scanner differed, we considered acquisition from the two scanners split into two separate cohorts (UNIBA1 and UNIBA2).

4.1.2. PNC. Participants and their caregivers rated lifetime psychopathology symptom items on the computerized version of GOASSESS, a structured interview, and an assessment that incorporates well-validated and reliable measures for psychopathology screening (39). Inclusion/exclusion criteria are described in *SI Appendix, section 1*. All study procedures were approved by the Institutional Review Board at the University of Pennsylvania. Briefly, written assent from youths and written informed consent from caregivers were obtained after they received a description of the study procedures.

4.1.3. ABCD. Participants and their caregivers completed a wide assessment including both physical and mental health information (82). Inclusion/exclusion criteria are described in *SI Appendix, section 1*. Most ABCD research sites rely on a central Institutional Review Board at the University of California, San Diego, for the ethical review and approval of the research protocol, with a few sites obtaining local Institutional Review Board approval.

4.1.4. UKB. Participants completed an extensive screening, including physical and mental health, through web-based questionnaires sent on a regular basis following the initial assessment. Inclusion and exclusion criteria are described in *SI Appendix, section 1*. UKB received ethical approval from the Research Ethics Committee (reference 11/NW/0382). All participants provided informed consent (<http://biobank.ctsu.ox.ac.uk/crystal/field.cgi?id=200>).

Age differences across groups between and within cohorts were assessed through separate Welch two-sample *t* tests. See *SI Appendix, section 1.1*, for a complete description of the analysis and results. All further analyses were corrected for age differences within age stages.

4.2. Experimental Procedure. For LIBD and UNIBA1, the experimental procedure was composed of a resting state, a blocked paradigm of the N-back task (54, 83), which measures increasing working memory loads, a blocked paradigm of an incidental declarative memory task, i.e., the Picture Encoding and Retrieval task (84–86), which dissociates specific encoding and retrieval processes. For the LIBD, we acquired a block design implicit emotion recognition task, i.e., the Faces Matching task (FMT) (87), while for UNIBA1, we used an event-related implicit emotion recognition task based on the gender recognition in human faces (88).

For UNIBA2, the experimental procedure was composed of a resting state, a blocked paradigm of the N-back task (54, 83), which was the same as the one acquired for the other two cohorts, an event-related paradigm of an explicit associative memory task, i.e., a revised version of the Relational and Item-Specific task (84), which dissociate specific encoding and retrieval processes, and a revised version of the event-related emotion recognition task used in the UNIBA1 cohort (89).

The experimental procedure in PNC was composed of a resting state, a fractal version of the standard N-back task (90), and a block design emotion identification task (91). For ABCD, the experimental procedure was composed of four short resting-state sessions (5 min each), and a revised version of the N-back task with emotional stimuli (92, 93). Finally, UKB included a resting state and the same emotion recognition paradigm used in LIBD, i.e., FMT (87). See *SI Appendix, sections 2–4*, for detailed information on neuropsychological tasks acquired during fMRI, MRI data acquisition, processing, and analysis.

4.3. Individual FNC Analysis. To estimate individual-level brain FNC features, we used the NeuroMark pipeline (41) on multiple fMRI scans including resting

state, working memory, episodic memory, and emotion recognition tasks. The ICA-based approach automatically and adaptively estimates individual-level ICs using prior network templates as guidance (41). We used the MOO-ICAR algorithm (44) available in the group ICA of fMRI toolbox (GIFT) (<http://trendscenter.org/software/>), by taking each participant's fMRI data as input. We used 53 labeled and ordered IC templates arranged into seven functional domains [e.g., auditory (N = 2 ICs), cerebellar (N = 4 ICs), cognitive control (N = 17 ICs), default mode (N = 7 ICs), sensorimotor (N = 9 ICs), subcortical (N = 5 ICs), and visual (N = 9 ICs)] as the spatial priors for guidance in estimating subject-specific networks (41).

We obtained whole-brain FNC estimates by computing Pearson's correlations between the time courses of each IC to yield an FNC matrix reflecting the relationship between any two IC for each fMRI session. In this FNC matrix, higher values correspond to higher connectivity between two IC time courses, whereas lower values correspond to lower connectivity between two IC time courses. We considered a spatial overlap of >75% between each IC spatial map and the whole-brain fMRI acquisition at the individual level to exclude the ICs that were not included in the individual fMRI image acquisition (94, 95). We obtained individual 53 × 53 matrices for each fMRI session performed by every participant, i.e., resting state, N-back, episodic memory encoding, episodic memory retrieval, and emotion recognition tasks. A vector of 1,370 FNC features was created by linearizing the FNC matrix for each participant for each session. Analyses were performed on age-, session-, and cohort-adjusted FNC *z* scores, which reflect the degree to which a participant's FNC deviates, in standard deviation units, from the normal value expected for their age and cohort based on observed NC groups data (96).

4.4. Effect of Age Group on Functional Connectivity. To study the FNC patterns associated with the age group, we first tested the age-group effect between neurotypical groups, i.e., yNC vs. oNC in the LIBD, UNIBA, and UNIBA2 cohorts independently, on the pairwise correlation coefficients between ICs. This was done separately for each IC through linear mixed-effect regressions on Fisher-*z* transformed correlation values (*R*²) between each IC pair (dependent variable: IC pair Pearson's correlation; fixed-effects: age group, session, sex, age group × session; age group × sex; relatedness index; random-effect: participants). We performed a 10,000-permutation test on the linear mixed-effects regressions independently for each cohort and determined differences across groups on the averaged IC pair Pearson's correlation across sessions. We considered reproducible the IC pairs that differed between groups, i.e., the main effect of the group across sessions, at empirical *p* value < 0.05 across cohorts. We accounted for multiple comparisons within each cohort through Benjamini-Hochberg (pFDR) significance correction (45). To obtain one *p* value estimate for each IC pair instead than one per cohort, we then combined reproducible effects via Fisher's combined probability test (97) using the *metap* package (98) implemented in R Statistics (<https://cran.r-project.org/>). We considered results significant with a two-tailed $\alpha = 0.05$. We also considered FNC differences during each session analyzed separately, i.e., the age group × session interaction. See *SI Appendix, section 6.2*.

To study the association between age-related neurotypical FNC patterns with behavioral performance, we tested the relationship between averaged FNC patterns across multiple fMRI acquisitions and i) hits and ii) RT at the working memory task, and iii) hits, and iv) RT weighted on the retrieval during the episodic memory task via separate Multiple Regression for each fMRI sessions for each NC group as well as via Linear Regressions for averaged FNC across fMRI sessions for each NC group. We combined *P* values derived from each cohort via Fisher's combined probability test (97) as described before to extract reproducible FNC × behavioral associations across all cohorts. We considered results significant with a two-tailed $\alpha = 0.05$. Additional control analyses on cognitive performance are reported in *SI Appendix, section 6.5*.

4.5. Effect of Familial or Clinical Risk and SCZ Diagnosis on Functional Connectivity. We investigated the effect of familial and, subsequently, clinical high risk on the FNC patterns of IC pairs resulting significantly associated with age. Differences between groups were tested via the Wilcoxon signed-rank test:

- yNC and ySIB in the LIBD cohort, to study the FNC alterations associated with the familial high risk of developing SCZ in the younger age range.

- oNC and oSIB in the LIBD and UNIBA1 cohorts, to study the FNC alterations associated with the familial risk of developing SCZ in the older age range.
- cNC and cSIB/FHR in the ABCD, to backtrace the FNC alterations associated with the familial high risk for SCZ during childhood
- yNC and yPSY in the UNIBA2 and PNC cohort, to study the FNC alterations associated with subthreshold symptoms of psychosis in the younger age range.
- cNC and cPSY in the PNC and ABCD, to backtrace the FNC alterations associated with subthreshold symptoms of psychosis during childhood

To check whether there was a difference between age-related FNC patterns in adulthood and the familial and, separately, clinical risk-related FNC, we compared via the Wilcoxon signed-rank test:

- oNC and ySIB in the LIBD cohort, to investigate whether the altered FNC patterns associated with the risk were different in oNC and to infer possible patterns of brain acceleration in the ySIB.
 - oNC and yPSY in the UNIBA2 cohort, to investigate the potential existence of FNC alterations associated with subthreshold clinical symptoms and whether the yPSY FNC profile differed from the one of oNC.
- Last, to investigate whether altered FNC patterns change in full-blown SCZ, we analyze differences between:

- oNC and oSCZ in LIBD, UNIBA1, and UNIBA2, to study possible FNC alterations associated with the diagnosis of SCZ.
- yNC and oSCZ in LIBD, UNIBA1, and UNIBA2, to investigate potential FNC alterations associated with diagnosis and to disentangle possible differences related to age.
- ySIB and oSCZ in the LIBD and UNIBA2 cohorts to analyze changes in brain maturation that persist (or not) also after the development of SCZ.
- yPSY and oSCZ in the UNIBA2 cohort to investigate whether FNC changes associated with the prodromal phase of psychosis are present also after the development of SCZ
- oSIB and oSCZ in the LIBD and UNIBA1 cohort, to investigate the differences in FNC between individuals that would not develop SCZ compared with patients at the same age stage.

To extract reproducible FNC differences ($pFDR < 0.05$) across all cohorts, we performed a 10,000-permutation test on the Wilcoxon signed-rank test within each cohort and combined reproducible effects via the Fisher's combined probability test (97) as described before (*Materials and Methods*, Section 4.4). The effect size (w) was calculated by dividing the z value extracted from the Wilcoxon signed-rank test by the square root of the number of observations independently for each cohort (99). Additional control analysis on gray matter structural differences across groups matching risk-related FNC patterns is reported in *SI Appendix, section 6.3*.

4.6. Association between Altered FNC Patterns and PRS. To examine the genetic substrate of altered FNC patterns significantly associated with risk, we investigated the relationship between averaged FNC across fMRI sessions with PRS (GWAS associations $P < 5 \times 10^{-8}$ to $P < 0.1$) (15) via separate multiple regression (dependent variable: IC pair Pearson's correlation; covariate of interest: PRS; nuisance covariates: age, risk/diagnosis groups, age groups, sex, and the first ten genomic eigenvariates), as well as between FNC for each fMRI sessions and PRS via separate multiple regression (dependent variable: IC pair Pearson's correlation; covariate of interest: PRS; nuisance covariates: age, risk/diagnosis groups, age groups, sex, and the first 10 genomic eigenvariates). See *SI Appendix, section 5*, for a detailed description of participants' genotype determination and PRS. The genomic eigenvariates were calculated through a principal component analysis on the genotypes of each SNP included in the PRS to exclude the effect of other population-related sources of variation, as already done by Chen et al. (20). To extract reproducible FNC \times PRS associations across all cohorts, we performed a mixed-effect model meta-analysis derived from partial regressions between FNC and PRS across cohorts through the metafor R package (100). Results were corrected for multiple comparisons through the Benjamini-Hochberg significance correction as the number of PRS tested ($k = 10$). We considered results significant with a two-tailed $\alpha = 0.05$.

Data, Materials, and Software Availability. All data needed to evaluate the conclusions in this work are present in the main text and/or *SI Appendix*. The group ICA Toolbox, NeuroMark template, as well as Matlab code used for the

FNC analysis are publicly available at the following link: <https://trendscenter.org/software/gift> (101). Data from UNIBA1 and UNIBA2 cannot be shared at the individual level in raw format because of ethical restrictions based on the protocol approved by the institutional ethics committee of the UNIBA to protect the privacy of the participants. Most data of the UNIBA2 cohort have been collected under the Marie Skłodowska-Curie grant agreement No 798181. The individual deidentified raw data from LIBD analyzed during this study are available from the corresponding author G.P. (giulio.pergola@libd.org) upon reasonable request. To ensure the replicability of the results reported in this work, individuals' aggregated data, summary statistics along with averaged and session-specific group FNC matrices, and related R and Matlab codes are available at: <https://doi.org/10.5281/zenodo.7948162> (102). This paper also analyzes existing, publicly available data upon approved requests. Accession numbers are reported in the *Acknowledgments* section.

ACKNOWLEDGMENTS. This project has received funding from the European Union's Horizon 2020 research and innovation program under the Marie Skłodowska-Curie grant agreement No 798181 awarded to G.P. (PI) and A.B., D.R.W.; from the European Union funding within the MUR PNRR Extended Partnership initiative on Neuroscience and Neuropharmacology (Project no. PE0000006 CUP H93C22000660006 "MNESYS, A multiscale integrated approach to the study of the nervous system in health and disease") to G.B., A.R., A.B., and G.P.; from the funding initiative Horizon Europe Seeds 2021 (Next Generation 8 EU-MUR D.M. 737/2021) for the project S68 CUP: H99J21017550006 to G.P. (PI) and L.A.A., G.B., A.R., A.B.; from the Apulian regional government for the project: "Early Identification of Psychosis Risk" to A.B.; from the Research Projects of National Relevance (PRIN) 2017 Prot. 2017K2NEF4 awarded to G.P.; from a Collaboration Grant from Exprivia Spa to G.P. under the ministerial decree D.M. n. 352/22 and A.B. under a collaboration agreement; from a Collaboration Grant from ITEL Telecomunicazioni Srl awarded to A.B.; from the 2021 Helmholtz Information and Data Science Academy Grant No. 12429 awarded to R.P. and J.D.; and from the NIH grant #R01MH118695 awarded to V.D.C. The collection of the MRI and genetic data for the LIBD cohort was supported by direct funding from the Intramural Research Program of the NIMH to the Clinical Brain Disorders Branch (PI: D.R.W., protocol 95-M-0150). The Philadelphia Neurodevelopmental Cohort (PNC; <https://www.med.upenn.edu/bbl/philadelphianeurodevelopmentalcohort.html>) is a research initiative funded by the NIMH through the American Reinvestment and Recovery Act of 2009. The initiative focuses on characterizing brain and behavior interaction with genetics. This is a collaborative research effort between the Brain Behavior Laboratory at the University of Pennsylvania and the Center for Applied Genomics at the Children's Hospital of Philadelphia (CHOP), led by Raquel E. Gur, MD, Ph.D. at the University of Pennsylvania and Hakon Hakonarson, MD, Ph.D., at the CHOP. Permission to use the PNC was provided to G.P. under project ID: 20998. UK Biobank (UKB; <https://www.ukbiobank.ac.uk>) is a large-scale biomedical database and research resource, containing in-depth genetic and health information from half a million UK participants. UKB was established by the Wellcome Trust medical charity, the Medical Research Council, the Department of Health, the Scottish Government, and the Northwest Regional Development Agency. It has also had funding from the Welsh Government, British Heart Foundation, Cancer Research UK, and Diabetes UK. UKB is supported by the National Health Service (NHS). UKB resource was provided to R.P. and J.D. under approved project ID: 41655 in the Institute of Neuroscience and Medicine-INM-7: Brain and Behavior at the Research Center Jülich. Data from the ABCD Study® (<https://abcdstudy.org>), held in the NIMH Data Archive (NDA), were obtained under approved request No 12036. The ABCD Study® is supported by the NIH and additional federal partners under award numbers U01DA041048, U01DA050989, U01DA051016, U01DA041022, U01DA051018, U01DA051037, U01DA050987, U01DA041174, U01DA041106, U01DA041117, U01DA041028, U01DA041134, U01DA050988, U01DA051039, U01DA041156, U01DA041025, U01DA041120, U01DA051038, U01DA041148, U01DA041093, U01DA041089, U24DA041123, and U24DA041147. A full list of supporters is available at <https://abcdstudy.org/federal-partners.html>. A listing of participating sites and a complete listing of the study investigators can be found at https://abcdstudy.org/consortium_members/. ABCD consortium investigators designed and implemented the study and/or provided

data but did not necessarily participate in the analysis or writing of this manuscript. The ABCD data repository grows and changes over time. The ABCD data used in this report came from NIMH Data Archive DOI: <https://doi.org/10.15154/1528793>. This manuscript reflects the views of the authors and may not reflect the opinions or views of the NIH, NHS, ABCD, UKB, and PNC investigators; the European Union and Research Executive Agency are not liable for any use that may be made of the information contained therein. No funding body intervened in the manuscript preparation. We would also like to thank Dr. Zening Fu, Mustafa Salman (TReNDS–Georgia State University, Georgia Institute of Technology, and Emory University), Annalisa Lella, Ciro Mazza, Rosa Barca, Riccarda Lomuscio (Department of Translational Biomedicine and Neuroscience, UNIBA), Prof. Simon Eickhoff (Institute of Neuroscience and Medicine, Brain and Behavior, Research Centre Jülich), Jan Kasper (Institute of Systems Neuroscience, Medical Faculty, Heinrich Heine University Düsseldorf), Dr. Alfonso Monaco (Department of Physics, UNIBA), Dr. Nora Penzel, Dr. Silvia Torretta (former Department of Basic Medical Science, Neuroscience, and Sense Organs, UNIBA), and Dr. Richard Straub (Lieber Institute for Brain Development, Johns Hopkins Medical Campus) for their help at different stages of this research. Finally, we thank all the volunteers who took part in the study.

Author affiliations: ^aDepartment of Translational Biomedicine and Neuroscience, University of Bari Aldo Moro, 70124 Bari, Italy; ^bTri-institutional Center for Translational Research in Neuroimaging and Data Science, Georgia State University, Georgia Institute of Technology, and Emory University, 30303 Atlanta, GA; ^cInstitute of Neuroscience and Medicine, Brain and Behavior, Research Centre Jülich, 52428 Jülich, Germany; ^dDepartment of Medicine and Surgery, Libera Università Mediterranea Giuseppe Degennaro, 70010 Casamassima, Italy; ^eLieber Institute for Brain Development, Johns Hopkins Medical Campus, 21205 Baltimore, MD; ^fPsychiatric Unit, University Hospital, 70124 Bari, Italy; ^gInstitute of Systems Neuroscience, Medical Faculty, Heinrich Heine University Düsseldorf, 40225 Düsseldorf, Germany; ^hDepartment of Neurology and Radiology, Johns Hopkins Medical Campus, 21287 Baltimore, MD; ⁱNeuroradiology Unit, Scientific Institute for Research, Hospitalization and Health Care, Casa Sollievo della Sofferenza, 71013 San Giovanni Rotondo, Foggia, Italy; ^jSection of Psychiatry, Department of Neuroscience, University of Padova, 35121 Padua, Italy; ^kDepartment of Mental Health, Azienda Sanitaria Locale Foggia, 71121 Foggia, Italy; ^lDepartment of Clinical and Experimental Medicine, University of Foggia, 71122 Foggia, Italy; ^mDepartment of Mental Health, Azienda Sanitaria Locale Barletta-Andria-Trani, 76123 Andria, Italy; ⁿDepartment of Mental Health, Azienda Sanitaria Locale Bari, 70132 Bari, Italy; ^oDepartment of Mental Health, Azienda Sanitaria Locale Brindisi, 72100 Brindisi, Italy; ^pDepartment of Psychiatry and Behavioral Sciences, Johns Hopkins University School of Medicine, 21205 Baltimore, MD; ^qDepartment of Neuroscience, Johns Hopkins University School of Medicine, 21287 Baltimore, MD; and ^rDepartment of Genetic Medicine, Johns Hopkins University School of Medicine, 21287 Baltimore, MD

Author contributions: R.P., A.B., V.D.C., and G.P. designed research; R.P., L.A.A., L.F., G.S., V.S.M., T.P., and the Apulian Network on Risk for Psychosis performed research; T.P.D. and V.D.C. contributed new reagents/analytic tools; R.P., G.P., G.S., L.S., G.C.K., and Q.C. analyzed data; L.A.A., F.S., A.B., V.D.C., and G.P. provided supervision; G.B., J.D., A.L.G., V.S.M., T.P., P.S., W.U., D.R.W., A.B., V.D.C., and G.P. contributed resources; and R.P., L.A.A., A.R., D.R.W., A.B., V.D.C., and G.P. wrote the paper.

- M. Arain *et al.*, Maturation of the adolescent brain. *Neuropsychiatr Dis. Treat* **9**, 449–461 (2013).
- N. Gogtay *et al.*, Dynamic mapping of human cortical development during childhood through early adulthood. *Proc. Natl. Acad. Sci. U.S.A.* **101**, 8174–8179 (2004).
- C. Battista *et al.*, Mechanisms of interactive specialization and emergence of functional brain circuits supporting cognitive development in children. *NPJ Sci. Learn.* **3**, 1 (2018).
- T. Paus, M. Keshavan, J. N. Giedd, Why do many psychiatric disorders emerge during adolescence? *Nat. Rev. Neurosci.* **9**, 947–957 (2008).
- D. R. Weinberger, Implications of normal brain development for the pathogenesis of schizophrenia. *Arch. Gen. Psychiatry* **44**, 660–669 (1987).
- P. D. McGorry, Beyond psychosis risk: Early clinical phenotypes in mental disorder and the subthreshold pathway to safe, timely and effective care. *Psychopathology* **47**, 285–286 (2014).
- O. Miranda-Dominguez *et al.*, Heritability of the human connectome: A connectotyping study. *Netw. Neurosci.* **2**, 175–199 (2018).
- L. T. Elliott *et al.*, Genome-wide association studies of brain imaging phenotypes in UK Biobank. *Nature* **562**, 210–216 (2018).
- D. V. Demeter *et al.*, Functional connectivity fingerprints at rest are similar across youths and adults and vary with genetic similarity. *iScience* **23**, 100801 (2020).
- Y. He *et al.*, Organized resting-state functional connectivity of the prefrontal cortex in patients with schizophrenia. *Neuroscience* **446**, 14–27 (2020).
- D. J. Holt *et al.*, Abnormalities in personal space and parietal-frontal function in schizophrenia. *Neuroimage Clin.* **9**, 233–243 (2015).
- B. Hahn, B. M. Robinson, C. J. Leonard, S. J. Luck, J. M. Gold, Posterior parietal cortex dysfunction is central to working memory storage and broad cognitive deficits in schizophrenia. *J. Neurosci.* **38**, 8378–8387 (2018).
- L. Fusar-Poli *et al.*, Examining facial emotion recognition as an intermediate phenotype for psychosis: Findings from the EUGEI study. *Prog. Neuropsychopharmacol. Biol. Psychiatry* **113**, 110440 (2021).
- L. A. Antonucci *et al.*, Multivariate classification of schizophrenia and its familial risk based on load-dependent attentional control brain functional connectivity. *Neuropsychopharmacology* **45**, 613–621 (2020).
- S. M. Purcell *et al.*, International Schizophrenia Consortium, Common polygenic variation contributes to risk of schizophrenia and bipolar disorder. *Nature* **460**, 748–752 (2009).
- V. Trubetskoy *et al.*, Mapping genomic loci implicates genes and synaptic biology in schizophrenia. *Nature* **604**, 502–508 (2022).
- I. I. Gottesman, J. Shields, A polygenic theory of schizophrenia. *Proc. Natl. Acad. Sci. U.S.A.* **58**, 199–205 (1967).
- J. A. Miller *et al.*, Effects of schizophrenia polygenic risk scores on brain activity and performance during working memory subprocesses in healthy young adults. *Schizophr. Bull.* **44**, 844–853 (2018).
- J. Chen *et al.*, Variability in resting state network and functional network connectivity associated with schizophrenia genetic risk: A pilot study. *Front. Neurosci.* **12**, 114 (2018).
- Q. Chen *et al.*, Schizophrenia polygenic risk score predicts mnemonic hippocampal activity. *Brain* **141**, 1218–1228 (2018).
- M. L. Elliott *et al.*, What is the test-retest reliability of common task-functional MRI measures? New empirical evidence and a meta-analysis. *Psychol. Sci.* **31**, 792–806 (2020).
- M. L. Elliott, A. R. Knodt, A. R. Hariri, Striving toward translation: Strategies for reliable fMRI measurement. *Trends Cogn. Sci.* **25**, 776–787 (2021).
- E. S. Finn *et al.*, Functional connectome fingerprinting: Identifying individuals using patterns of brain connectivity. *Nat. Neurosci.* **18**, 1664–1671 (2015).
- R. M. Birn *et al.*, The effect of scan length on the reliability of resting-state fMRI connectivity estimates. *Neuroimage* **83**, 550–558 (2013).
- M. L. Elliott *et al.*, General functional connectivity: Shared features of resting-state and task fMRI drive reliable and heritable individual differences in functional brain networks. *Neuroimage* **189**, 516–532 (2019).
- M. W. Cole, D. S. Bassett, J. D. Power, T. S. Braver, S. E. Petersen, Intrinsic and task-evoked network architectures of the human brain. *Neuron* **83**, 238–251 (2014).
- A. Bertolino, G. Blasi, The genetics of schizophrenia. *Neuroscience* **164**, 288–299 (2009).
- A. Meyer-Lindenberg, D. R. Weinberger, Intermediate phenotypes and genetic mechanisms of psychiatric disorders. *Nat. Rev. Neurosci.* **7**, 818–827 (2006).
- F. Sambataro *et al.*, Normal aging modulates prefrontal-parietal networks underlying multiple memory processes. *Eur. J. Neurosci.* **36**, 3559–3567 (2012).
- M. S. Cetin *et al.*, Thalamic and posterior temporal lobe show greater inter-network connectivity at rest and across sensory paradigms in schizophrenia. *Neuroimage* **97**, 117–126 (2014).
- F. Sambataro *et al.*, Age-related alterations in default mode network: Impact on working memory performance. *Neurobiol. Aging* **31**, 839–852 (2010).
- V. D. Calhoun, T. Adali, G. D. Pearlson, J. J. Pekar, A method for making group inferences from functional MRI data using independent component analysis. *Hum. Brain Mapp.* **14**, 140–151 (2001).
- M. S. Keshavan *et al.*, Premorbid cognitive deficits in young relatives of schizophrenia patients. *Front. Hum. Neurosci.* **3**, 62 (2010).
- M. R. Broome *et al.*, Delusional ideation, manic symptomatology and working memory in a cohort at clinical high-risk for psychosis: A longitudinal study. *Eur. Psychiatry* **27**, 258–263 (2012).
- P. Fusar-Poli *et al.*, The psychosis high-risk state: A comprehensive state-of-the-art review. *JAMA Psychiatry* **70**, 107–120 (2013).
- Y. Chung *et al.*, Use of machine learning to determine deviance in neuroanatomical maturity associated with future psychosis in youths at clinically high risk. *JAMA Psychiatry* **75**, 960–968 (2018).
- T. Hajek *et al.*, Brain age in early stages of bipolar disorders or schizophrenia. *Schizophr. Bull.* **45**, 190–198 (2019).
- M. Truelove-Hill *et al.*, A multidimensional neural maturation index reveals reproducible developmental patterns in children and adolescents. *J. Neurosci.* **40**, 1265–1275 (2020).
- M. E. Calkins *et al.*, The Philadelphia neurodevelopmental cohort: Constructing a deep phenotyping collaborative. *J. Child Psychol. Psychiatry* **56**, 1356–1369 (2015).
- T. Kaufmann *et al.*, Delayed stabilization and individualization in connectome development are related to psychiatric disorders. *Nat. Neurosci.* **20**, 513–515 (2017).
- Y. Du *et al.*, NeuroMark: An automated and adaptive ICA based pipeline to identify reproducible fMRI markers of brain disorders. *Neuroimage Clin.* **28**, 102375 (2020).
- A. Polari *et al.*, Clinical trajectories in the ultra-high risk for psychosis population. *Schizophr. Res.* **197**, 550–556 (2018).
- G. Pergola *et al.*, Consensus molecular environment of schizophrenia risk genes in coexpression networks shifting across age and brain regions. *Sci. Adv.* **9**, eade2812 (2023).
- Y. Du, Y. Fan, Group information guided ICA for fMRI data analysis. *Neuroimage* **69**, 157–197 (2013).
- Y. Benjamini, Y. Hochberg, Controlling the false discovery rate: A practical and powerful approach to multiple testing. *J. R. Stat. Soc.* **57**, 289–300 (1995).
- M. Edde, G. Leroux, E. Altena, S. Chanraud, Functional brain connectivity changes across the human life span: From fetal development to old age. *J. Neurosci. Res.* **99**, 236–262 (2021).
- M. W. Cole, T. Ito, C. Cocuzza, R. Sanchez-Romero, The functional relevance of task-state functional connectivity. *J. Neurosci.* **41**, 2684–2702 (2021).
- H. I. Zonneveld *et al.*, Patterns of functional connectivity in an aging population: The rotterdam study. *Neuroimage* **189**, 432–444 (2019).
- S. M. Kolk, P. Rakic, Development of prefrontal cortex. *Neuropsychopharmacology* **47**, 41–57 (2022).
- E. Ankudowich, S. Pasvanis, M. N. Rajah, Changes in the correlation between spatial and temporal source memory performance and BOLD activity across the adult lifespan. *Cortex* **91**, 234–249 (2017).
- P. Mirino *et al.*, Cerebellum-cortical interaction in spatial navigation and its alteration in dementias. *Brain Sci.* **12**, 523 (2022).
- J. D. Schmahmann, The cerebellum and cognition. *Neurosci. Lett.* **688**, 62–75 (2019).
- R. Cabeza, N. D. Anderson, J. K. Locantore, A. R. McIntosh, Aging gracefully: Compensatory brain activity in high-performing older adults. *Neuroimage* **17**, 1394–1402 (2002).
- J. H. Callicott *et al.*, Physiological dysfunction of the dorsolateral prefrontal cortex in schizophrenia revisited. *Cereb Cortex* **10**, 1078–1092 (2000).
- A. Bertolino *et al.*, Specific relationship between prefrontal neuronal N-acetylaspartate and activation of the working memory cortical network in schizophrenia. *Am. J. Psychiatry* **157**, 26–33 (2000).
- J. R. Cohen, M. D'Esposito, The segregation and integration of distinct brain networks and their relationship to cognition. *J. Neurosci.* **36**, 12083–12094 (2016).

57. V. Y. Wang, H. Y. Zoghbi, Genetic regulation of cerebellar development. *Nat. Rev. Neurosci.* **2**, 484–491 (2001).
58. C. Limperopoulos *et al.*, Injury to the premature cerebellum: Outcome is related to remote cortical development. *Cereb Cortex* **24**, 728–736 (2014).
59. S. S. Wang, A. D. Kloth, A. Badura, The cerebellum, sensitive periods, and autism. *Neuron* **83**, 518–532 (2014).
60. K. Franke, C. Gaser, Ten years of BrainAGE as a neuroimaging biomarker of brain aging: What insights have we gained? *Front. Neurol.* **10**, 789 (2019).
61. M. Fabiani, It was the best of times, it was the worst of times: A psychophysiology's view of cognitive aging. *Psychophysiology* **49**, 283–304 (2012).
62. P. F. Sullivan, K. S. Kendler, M. C. Neale, Schizophrenia as a complex trait: Evidence from a meta-analysis of twin studies. *Arch. Gen. Psychiatry* **60**, 1187–1192 (2003).
63. A. Zalesky *et al.*, Delayed development of brain connectivity in adolescents with schizophrenia and their unaffected siblings. *JAMA Psychiatry* **72**, 900–908 (2015).
64. A. Bertolino *et al.*, Functional lateralization of the sensorimotor cortex in patients with schizophrenia: Effects of treatment with olanzapine. *Biol. Psychiatry* **56**, 190–197 (2004).
65. V. S. Mattay *et al.*, Abnormal functional lateralization of the sensorimotor cortex in patients with schizophrenia. *Neuroreport* **8**, 2977–2984 (1997).
66. A. Anticevic *et al.*, Early-course unmedicated schizophrenia patients exhibit elevated prefrontal connectivity associated with longitudinal change. *J. Neurosci.* **35**, 267–286 (2015).
67. S. Qi *et al.*, Derivation and utility of schizophrenia polygenic risk associated multimodal MRI frontotemporal network. *Nat. Commun.* **13**, 4929 (2022).
68. N. d. M. dell'Istruzione, Prot. N. 482 del 18.02.2021. Linee di Orientamento per la prevenzione e il contrasto del Bullismo e Cyberbullismo (2021).
69. G. Pergola, N. Penzel, L. Sportelli, A. Bertolino, Lessons learned from parsing genetic risk for schizophrenia into biological pathways. *Biol. Psychiatry* **94**, 121–130 (2022), 10.1016/j.biopsych.2022.10.009.
70. E. F. Walker, Developmentally moderated expressions of the neuropathology underlying schizophrenia. *Schizophr. Bull.* **20**, 453–480 (1994).
71. T. M. Hyde *et al.*, Enuresis as a premorbid developmental marker of schizophrenia. *Brain* **131**, 2489–2498 (2008).
72. I. Falkenberg *et al.*, Failure to deactivate medial prefrontal cortex in people at high risk for psychosis. *Eur. Psychiatry* **30**, 633–640 (2015).
73. P. Fusar-Poli *et al.*, Spatial working memory in individuals at high risk for psychosis: Longitudinal fMRI study. *Schizophr. Res.* **123**, 45–52 (2010).
74. J. van Os *et al.*, Schizophrenia and the environment: Within-person analyses may be required to yield evidence of unconfounded and causal association—the example of cannabis and psychosis. *Schizophr. Bull.* **47**, 594–603 (2021).
75. O. D. Howes *et al.*, Pathways to schizophrenia: The impact of environmental factors. *Int. J. Neuropsychopharmacol.* **7** (suppl. 1), S7–S13 (2004).
76. J. van Os *et al.*, European Network of National Networks studying Gene-Environment Interactions in Schizophrenia (EU-GEI). Identifying gene-environment interactions in schizophrenia: Contemporary challenges for integrated, large-scale investigations. *Schizophr. Bull.* **40**, 729–736 (2014).
77. G. Pergola *et al.*, Evocative gene-environment correlation between genetic risk for schizophrenia and bullying victimization. *World Psychiatry* **18**, 366–367 (2019).
78. A. Lella, L. A. Antonucci, G. Pergola, The interpretation of discrepancies between peer victimization experiences reported by different informants in capturing victimization-related genetic liability. A commentary on Armitage *et al.* (2022). *JCPP Adv.* **3**, e12137 (2023).
79. G. E. Woolway *et al.*, Schizophrenia polygenic risk and experiences of childhood adversity: A systematic review and meta-analysis. *Schizophr. Bull.* **48**, 967–980 (2022).
80. O. D. Howes, R. M. Murray, Schizophrenia: An integrated sociodevelopmental-cognitive model. *Lancet* **383**, 1677–1687 (2014).
81. C. C. Bell, DSM-IV: Diagnostic and statistical manual of mental disorders. *JAMA* **272**, 828–829 (1994).
82. D. M. Barch *et al.*, Demographic and mental health assessments in the adolescent brain and cognitive development study: Updates and age-related trajectories. *Dev. Cogn. Neurosci.* **52**, 101031 (2021).
83. A. Bertolino *et al.*, Prefrontal dysfunction in schizophrenia controlling for COMT Val158Met genotype and working memory performance. *Psychiatry Res.* **147**, 221–226 (2006).
84. J. D. Ragland *et al.*, Relational and item-specific encoding (RISE): Task development and psychometric characteristics. *Schizophr. Bull.* **38**, 114–124 (2012).
85. A. Di Giorgio *et al.*, Evidence that hippocampal-parahippocampal dysfunction is related to genetic risk for schizophrenia. *Psychol. Med.* **43**, 1661–1671 (2013).
86. R. Rasetti *et al.*, Altered hippocampal-parahippocampal function during stimulus encoding: A potential indicator of genetic liability for schizophrenia. *JAMA Psychiatry* **71**, 236–247 (2014).
87. H. Cao *et al.*, Altered functional subnetwork during emotional face processing: A potential intermediate phenotype for schizophrenia. *JAMA Psychiatry* **73**, 598–605 (2016).
88. G. Blasi *et al.*, Functional variation of the dopamine D2 receptor gene is associated with emotional control as well as brain activity and connectivity during emotion processing in humans. *J. Neurosci.* **29**, 14812–14819 (2009).
89. P. Taurisano *et al.*, DAT by perceived MC interaction on human prefrontal activity and connectivity during emotion processing. *Soc. Cogn. Affect Neurosci.* **8**, 855–862 (2013).
90. J. D. Ragland *et al.*, Working memory for complex figures: An fMRI comparison of letter and fractal n-back tasks. *Neuropsychology* **16**, 370–379 (2002).
91. R. C. Gur *et al.*, Brain activation during facial emotion processing. *Neuroimage* **16**, 651–662 (2002).
92. D. M. Barch *et al.*, Function in the human connectome: Task-fMRI and individual differences in behavior. *Neuroimage* **80**, 169–189 (2013).
93. A. O. Cohen *et al.*, The impact of emotional states on cognitive control circuitry and function. *J. Cogn. Neurosci.* **28**, 446–459 (2016).
94. A. Fornito, J. Yoon, A. Zalesky, E. T. Bullmore, C. S. Carter, General and specific functional connectivity disturbances in first-episode schizophrenia during cognitive control performance. *Biol. Psychiatry* **70**, 64–72 (2011).
95. L. Geerligs, C. Cam, R. N. Henson, Functional connectivity and structural covariance between regions of interest can be measured more accurately using multivariate distance correlation. *Neuroimage* **135**, 16–31 (2016).
96. H. K. Hamilton *et al.*, Mismatch negativity in response to auditory deviance and risk for future psychosis in youth at clinical high risk for psychosis. *JAMA Psychiatry* **79**, 780–789 (2022).
97. R. A. Fisher, *Statistical Methods for Research Workers* (Oliver and Boyd, Edinburgh, 1925).
98. S. Balduzzi, G. Rucker, G. Schwarzer, How to perform a meta-analysis with R: A practical tutorial. *Evid. Based Ment. Health* **22**, 153–160 (2019).
99. R. R. Rosenthal, D. B., Comparing effect sizes of independent studies. *Psychol. Bull.* **92**, 500–504 (1982).
100. W. Viechtbauer, Conducting meta-analyses in R with the metafor Package. *J. Stat. Softw.* **36**, 1–48 (2010).
101. R. Srinivas, J. H. Bockolt, V. D. Callhoun, Group ICA Toolbox (GIFT and EEGIFT). NITRC. <https://www.nitrc.org/projects/gift/>. Deposited 4 September 2007.
102. P. Roberta *et al.*, Changes in patterns of age-related network connectivity are associated with risk for schizophrenia (1.1) [Data set]. Zenodo. <https://doi.org/10.5281/zenodo.7948162>. Deposited 21 April 2023.